

Project: **1258**

Project title: **RETAKE—Carbon Dioxide Removal by Alkalinity Enhancement: Potential, Benefits and Risks**

Principal investigator: **Ute Daewel**

Report period: **2023-11-01 to 2024-10-31**

The report of the outcome from the last year are divided into two parts:

- 1) we have furthered the understanding of the ocean alkalinity enhancement (OAE) effects on the North Sea by analysing the results of the scenario simulations by adding alkalinity to the seawater surface across various deployment sites (as shown in Fig. 1A). A fixed amount of alkalinity (134Gmol/year) was added as a continuous flux across the surface boundary of the selected sites.

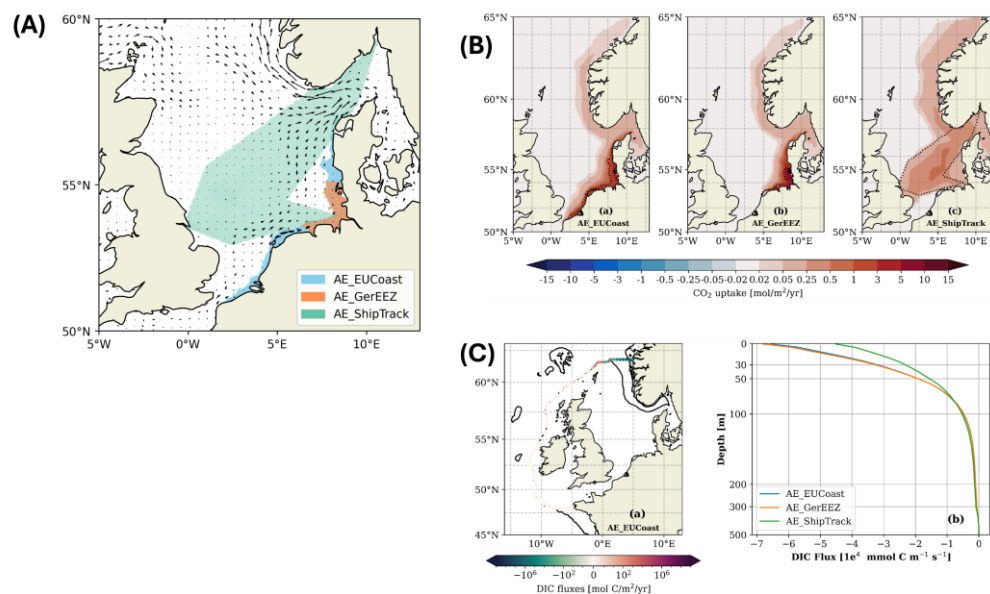


Fig.1 (A) Sites of the AE deployments, parts of the sites are overlapped. (B) The spatial distribution of excess  $\text{CO}_2$  uptake averaged over 2002-2010 for the three OAE scenarios. Note the nonlinear color bar. (C)-(a) Difference of the vertically integrated DIC flux per unit horizontal distance across the shelf-break relative to the CTL run for the AE\_EUCoast scenario in 2010. Positive values indicate flux in the on-shelf direction. Black contour shows the 200m isobath. (b) Difference of the DIC flux per unit depth ( $\text{m}^2/\text{s}$ ) over the northern gate relative to the CTL run for the three scenarios in 2010. Negative values indicate DIC export to the Atlantic Ocean.

The areas where excess  $\text{CO}_2$  uptake is detected extends from the deployment sites to the Skagerrak and the Norwegian Trench (Fig. 1B). The maximum flux is observed at the deployment site, with the magnitude varying among the three scenarios according to the flux of alkalinity addition. The AE\_ShipTrack scenario, having the lowest maximum  $\text{CO}_2$  uptake flux, is featured by the largest spatial scale of detectable uptake flux compared to the other two scenarios, with the  $\text{CO}_2$  uptake flux of  $0.25 \text{ mol}/\text{m}^2/\text{yr}$  extending into the North Atlantic up to  $65^\circ\text{N}$ .

OAE does not cause significant changes in off-shelf DIC export across most of the shelf break. Notable changes are observed only in the section near Shetland and the northern gate spanning the Norwegian Trench (Fig. 1C(a)). In the northern part of the shelf near Shetland, OAE leads to an increase in DIC transport onto the shelf, while across the Norwegian Trench, DIC export increases due to the enhanced  $\text{CO}_2$  sequestration. To assess variability with depth, we summed the DIC fluxes along the transect across the Norwegian Trench. The resulting depth profile (Fig. 1C(b)) displays greater export in the AE\_EUCoast and AE\_GerEEZ scenarios in the upper 80 meters. Below this depth, the enhanced export is similar across all scenarios, with the AE\_ShipTrack scenario showing a slightly larger export.

From this set of simulations, we conclude that the choice of OAE deployment sites is critical in term of both the  $\text{CO}_2$  uptake and the concurrent shifts in the carbon chemistry, which might bring potential risks to the ecosystems. Spreading alkalinity over a larger coastal area (the European coast) and a smaller area (the German EEZ) result in similar OAE efficiency. However, concentrating alkalinity in the smaller German EEZ area significantly alters the carbon chemistry, resulting in a pH change more than twice as great as that observed with deployment along the European coast. While this approach reduces OAE costs and enhances  $\text{CO}_2$  offset, it increases the risk to the local ecosystem. Dispersing the

material over a larger offshore area, such as the ship track area, leads to greater alkalinity loss to deeper waters. With less alkalinity available at the surface, CO<sub>2</sub> uptake is reduced. However, long-term DIC storage remains comparable to that of coastal deployments, resulting in similar DIC transport efficiency to the open ocean. In this scenario, the local water undergoes the least change in carbon chemistry, with alterations an order of magnitude smaller than in the other two scenarios.

This part of results has been composed of a manuscript which is ready to submit to 'Earth's Future'.

- 2) We further simulated the olivine weathering in a more realistic manner by taking into consideration the effect of sediment types. For this, we targeted three sediment types: a) In the bedload application/scenario, we applied olivine on top of the sediment, in areas with high hydrodynamic energy. The idea was that during bedload transport of sediment particles, the sediment particles crash into the deposited olivine causing a natural grinding effect, leading to a smaller grain size and thus faster dissolution rate. We utilized a grain size of 120  $\mu\text{m}$  (relatively large for marine enhanced rock weathering but small considering the surrounding sediment) as grinding to this grainsize is very cost efficient. The pH was assumed to equal the water pH as the olivine is deposited on top of the sediment. The intrinsic dissolution rate constant, which was taken from experiments where this continuous grain to grain collision was simulated in bottles that were continuously tumbled/rotated. b) In the permeable application, olivine is mixed into the sediment, the dominant transport process in these sandy sediments is advective wave action. The idea here was that olivine dissolution is enhanced due to the lower sediment pH compared to the overlying water. Dissolution products were assumed not to build up, as advection flushes the porewater. We utilized a grain size of 120  $\mu\text{m}$  as well, which is comparable with the finest fraction of sand. c) In the cohesive application, olivine is mixed into muddy/silty cohesive sediments. The main transport processes at play here are bioturbation, which were assumed to prevent porewater saturation. Since cohesive sediments are also smaller grain size wise, we can also apply finer olivine here. We utilized a  $\sim 29 \mu\text{m}$  grain size which is the median grain size for the silt. The necessary parameters were provided by L. Geerts from the University of Antwerp (in support of Project 'DE-HEAT').

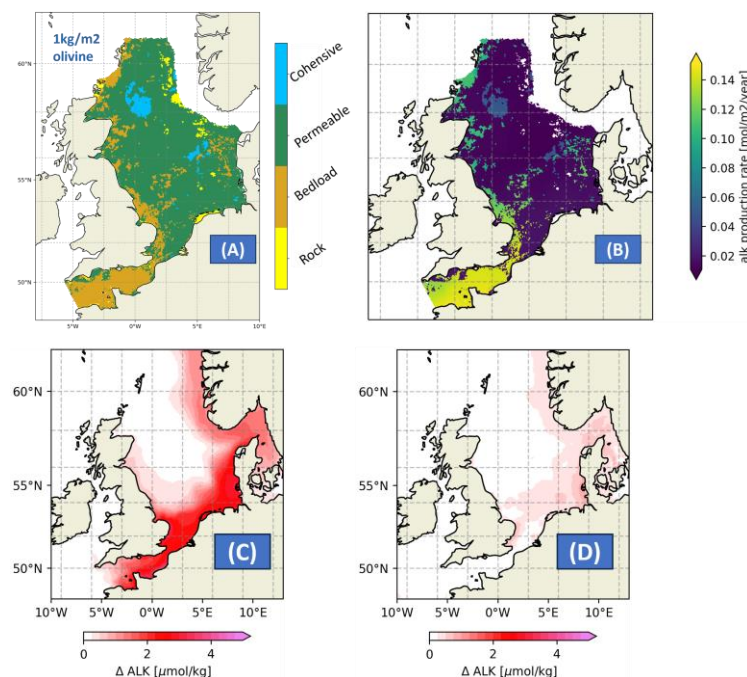


Fig.2 (A) the map of the sediment types. Note here rock areas are not considered in the scenario. (B) the rate of alkalinity production due olivine weathering. (C) the increase in the surface alkalinity in the last simulation year (2010) due to the bedload type of olivine weathering. (D) the increase in the surface alkalinity in the last simulation year (2010) due to the permeable type of olivine weathering.

In this scenario, 1 kg/m<sup>2</sup> of olivine was added to the sediment, with initial grain size varying according to sediment types (Fig. 2A). The model ran from 2001 to 2010. As shown in Fig. 2B, bedload sediments produce the most alkalinity due to their higher olivine dissolution rate, while permeable sediments release the least alkalinity, primarily due to larger grain sizes and a relatively low intrinsic dissolution rate. In bedload sediment areas, alkalinity production follows a north-to-south gradient, largely driven by temperature differences. The bedload type contributes the most to surface alkalinity, nearly an order of magnitude higher than the permeable type. Alkalinity transport follows the general circulation pattern, with the highest surface alkalinity increase detected along the European coast, despite a significant portion of the bedload sediment being near the British coast, where alkalinity concentrations remain largely unchanged.

This work will be continued in the next year in the frame of future projection to investigate the long-term effect of olivine weathering.